

Research Article

Synthesis, Structural Characterization, Degradation Rate, and Biocompatibility of Magnesium-Carbonate Apatite (Mg-CO₃Ap) Composite and Its Potential as Biodegradable Orthopaedic Implant Base Material

Ahmad Jabir Rahyussalim ¹, Aldo Fransiskus Marsetio ¹, Achmad Fauzi Kamal ¹,
Sugeng Supriadi ², Iwan Setyadi ², Pancar Muhammad Pribadi,² Wildan Mubarak ³,
and Tri Kurniawati ⁴

¹Department of Orthopaedic and Traumatology, Faculty of Medicine Universitas Indonesia - Cipto Mangunkusumo National Central General Hospital, Jakarta 10340, Indonesia

²Department of Mechanical Engineering, Faculty of Engineering Universitas Indonesia, Jakarta, Depok, West Java 16424, Indonesia

³Division of Chemical Engineering, Department of Materials Engineering Science, Graduate School of Engineering Science, Osaka University, Toyonaka, Osaka 560-8531, Japan

⁴Stem Cells and Tissues Engineering Research Cluster, Indonesian Medical Education and Research Institute-Faculty of Medicine Universitas Indonesia, Jakarta 10340, Indonesia

Correspondence should be addressed to Aldo Fransiskus Marsetio; aldofransiskus@gmail.com

Received 15 December 2020; Revised 19 February 2021; Accepted 2 March 2021; Published 19 March 2021

Academic Editor: Hassan Karimi-Maleh

Copyright © 2021 Ahmad Jabir Rahyussalim et al. This is an open access article distributed under the Creative Commons Attribution License, which permits unrestricted use, distribution, and reproduction in any medium, provided the original work is properly cited.

Suitable biomechanical properties with a degradation rate parallel to normal bone healing time are vital characteristics for biodegradable implant material in orthopaedics. Magnesium (Mg) is a natural micronutrient as well as biodegradable metal with biomechanical characteristics close to that of the human bone, while carbonate apatite (CO₃Ap) is a biological apatite with good osteoconductivity which allows bone healing without forming fibrotic tissue. We fabricated a Mg-CO₃Ap composite with various content ratios by powder metallurgy, various milling times (3, 5, and 7 hours) at 200 RPM, warm compaction at 300°C and pressure of 265 MPa, sintering at 550°C, holding time of 1 hour, heating rate of 5°C/minutes, and room atmosphere cooling. Specimens were successfully created and had a density comparable to that of the human bone (1.95-2.13 g/cm³). Good biocompatibility was found on Mg-10% CO₃Ap composite (66.67% of viable cells). Nevertheless, its biomechanical properties and corrosion resistance were inferior to the human bone. Additionally, the materials of the composites make the surrounding environment alkaline. Interparticle consolidation and grain size were dissatisfactory due to microstructural pores presumably formed by the Mg(OH)₂ layer and oxidation process during sintering. However, alkaline condition caused by the material corrosion by-product might be beneficial for bone healing and wound healing process. Modifications on fabrication parameters are needed to improve interparticle consolidation, refine grain size, improve biomechanical strength, reduce corrosion products, and improve the degradation rate.

1. Introduction

A biomaterial is a material that has been processed to be biocompatible when implanted in the human body and able to

support or replace the function of an organ [1, 2]. Metallic implants are commonly used in orthopaedic cases to aid in restoring function or to replace damaged bone tissue [2]. The essential prerequisites of a biomaterial for an orthopaedic

implant include good biocompatibility and durability, wear and stress resistance, preventive of biocorrosion and aseptic loosening, does not instigate adverse immune response, and supports bone bioactivity and osteoconduction [3].

The most commonly used metallic biomaterials are stainless steel, titanium alloy (Ti-6Al-4V), and chromium cobalt alloy. The use of a metallic implant has its common problem: the vast difference of Young modulus between the implant and the bone. This difference may lead to stress shielding effect in which less stress is absorbed by the bone and bring about bone resorption [4]. Recent studies are trending towards the biodegradable capability of orthopaedic implant materials. A biodegradable implant is perhaps financially, psychologically, clinically, and culturally more preferable, considering the less need for implant removal.

Biodegradable material for an orthopaedic implant must fulfil some requirements, such as the degradation rate must be in line with fracture healing timeline, reduction of mechanical strength must conform with tissue healing, biocompatible, and minimal inflammation or immune reaction [5]. Ding stated some principles in designing material composite for an orthopaedic implant, namely, safe and biocompatible, yield strength of at least >200 MPa, elongation of $>10\%$, degradation rate of <0.5 mm/year on simulated body fluid at 37°C (so that the material can survive up to 90-180 days), and controlled and uniform degradation [6].

Inside our body, magnesium (Mg) is an important micronutrient, in which about 250-300 mg is acquired from daily food intake and stored in bone. The element plays important role in energy metabolism and function of organs such as the heart, muscles, nerves, bones, and kidney [7]. In the environment, Mg is also a biodegradable metal. It has biomechanical properties close to the bone. Mg has a Young modulus of 41-45 GPa and density of $1.74\text{-}1.84$ g/cm³ [8].

Carbonate apatite (CO_3Ap) is an inorganic apatite that can be found naturally in human bone. One study by Ayukawa et al. [9] found that CO_3Ap has high osteoconductivity and can induce bone healing without fibrotic tissue formation and, therefore, similar to the natural process of bone healing. Additionally, this material can be absorbed and replaced completely by new bone tissue by 1-1.5 years.

Our study examined and fabricated the magnesium and carbonate apatite composite. The outcome is expected to be able to have mechanical properties similar to or higher than the bone's and good osseointegration, improve bone osteoconductivity, be biocompatible, and induce minimal immunological reaction and toxicity. Eventually, the material would be considered a biodegradable orthopaedic implant that can be used for supporting bone.

2. Materials and Methods

2.1. Composite Fabrication. The powder metallurgy method was used by dry mixing Mg powder and CO_3Ap powder. Specimens with various content ratios of CO_3Ap were produced, namely, 100:0 (pure Mg), 95:5 (Mg-5CA), 90:10 (Mg-10CA), and 85:15 (Mg-15CA). Mixing was done with a planetary ball mill at 200 RPM, without lubricant. Vacuum drying at 200°C for 12 hours was applied to reduce water con-

tent and prevent oxidation reaction ($\text{Mg}(\text{OH})_2$). The powders were then put in a press die and compacted with hydraulic stamping in a muffle furnace at 265 MPa and temperature of 350°C . Composites were made in the form of miniplates (for biomechanical testing) and cylinder blocks (for biocompatibility and corrosion testing).

2.2. Mechanical Testing. The specimen for mechanical testing was made in the form of miniplates, sized $3 \times 0.5 \times 0.25$ cm. A three-point contact bending test was done on 10 samples (5 of pure Mg and 5 of Mg-5CA) according to ASTM E290-14 [10]. Data of flexural stress (σ_f), flexural strain (ϵ_f), and flexural elasticity modulus (E_f) were obtained.

2.3. Biocompatibility Tests. Biocompatibility tests were done *in vitro* by a direct contact method and MTT assay method. Cylindrical-shaped specimens (diameter of 10 mm, height 5 mm) were cut from a cylinder block. The milling time was varied for 3 hours, 5 hours, and 7 hours. The specimens were sterilized with an autoclave (121°C for 1 hour). On the direct contact method, specimens were put in a 12-well plate filled with a complete medium which has been filled by umbilical cord stem cell (UC-MSC) culture. Complete medium was mixed based on the mixing formulae by Pawitan et al. [11], which consists of Gibco[®] α -MEM powder (Thermo Fisher Scientific, Massachusetts, USA), penicillin-streptomycin 10,000 U/mL Gibco[®] Pen Strep (Thermo Fisher Scientific, Massachusetts, USA), Gibco[®] Amphotericin B 250 $\mu\text{g}/\text{mL}$ (Thermo Fisher Scientific, Massachusetts, USA), 1% L-Glutamine Gibco[®] GlutaMAX[™]-I (Thermo Fisher Scientific, Massachusetts, USA), and 10% thrombocyte concentrate (Indonesian Red Cross). The condition of cells in the medium was observed under an optical microscope with 4x magnification every 24 hours. One millilitre of the resuspended medium was stained with trypan blue and put in a hemacytometer. Living cells were observed and counted manually.

An indirect test using the MTT assay was done in accordance with the method used by Mosmann [12]. The colourimetric method was principally divided into three stages. Firstly, specimens were incubated in a cell-containing medium for 24 hours. Afterwards, the 24-hour-incubated specimens were moved into a new well containing fresh new cell-containing medium and incubated for a further 48 hours. After being incubated for 24 + 48 hours, the specimens were then moved into a new well containing fresh new cell-containing medium and incubated for a further 72 hours. Incubation was done in an incubator with temperature of 37°C and 5% CO_2 . Next, the medium was then mixed with cultured UC-MSC-containing complete medium in a 96-well plate with MTT solution (Vybrant[®] MTT Cell Proliferation Assay Kit, Thermo Fisher Scientific, Massachusetts, USA) and incubated again for a further 4 hours. After the incubation period, purple-coloured formazan crystal would form. The crystals are not solvable in aqueous solution. A nightly incubation process in the humid atmosphere was done. The higher the number of living cells, the higher the total metabolic activity. Thus, more formazan crystals were going



FIGURE 1: Fabricated composite specimens: (a) cylinder block; (b) cut specimen for biocompatibility test; (c) specimen for biomechanical test.

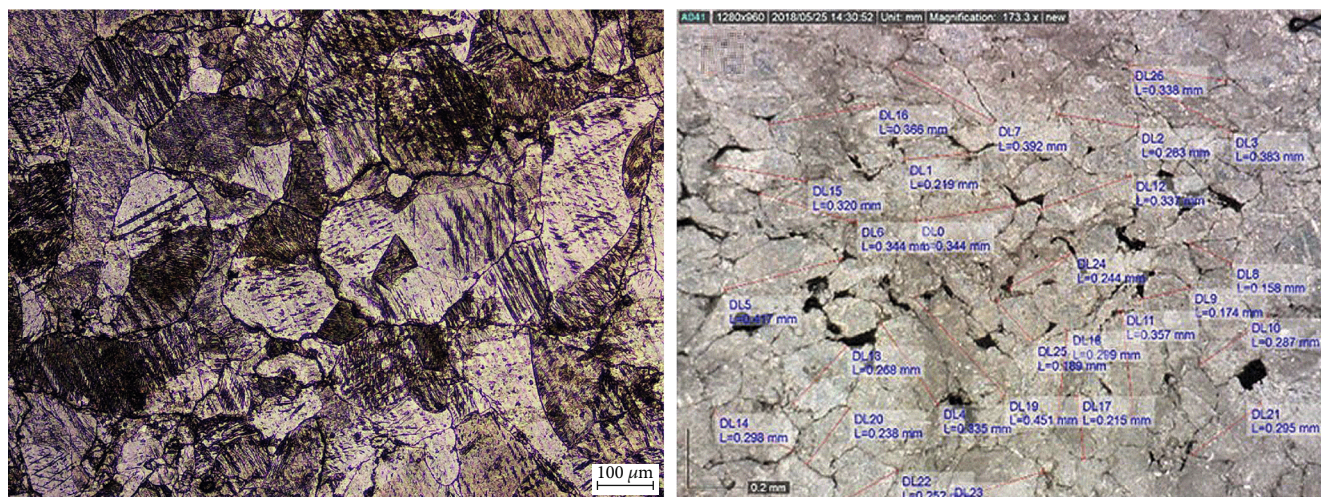


FIGURE 2: Optical microscope appearance of specimens. At magnification of 173x, pores within the material can be observed.

to be formed. Colour intensity generated by the formazan crystals was read by a spectrophotometer at 540 nm wavelength.

The biocompatibility experiment was done twice. The first experiment analysed specimens with different milling times, while the second experiment reanalysed the specimen which has the least toxicity profile on the first test.

2.4. Biocorrosion and Acidity Tests. An *in vitro* degradation test was conducted using Dulbecco's modified Eagle's medium (DMEM) (Biowest, Nuaille, France), at atmospheric condition, temperature of $37 \pm 0.5^\circ\text{C}$, and nonsterile and static condition. Steps of the corrosion test were done by

adapting ASTM G31-72 (2004) [13] and methods by Gonzalez et al. [14] Before the procedure, all of the specimens' dimensions, surface area, and weight were measured. Data of volume and density was acquired. The minimal volume of DMEM was 20–40 mL/cm².

The corrosion rate of extruded pure magnesium in a study by Liu et al. was used as a reference (0.6 mm/year = 23.64 mils/year) [15]. Minimum time of immersion was calculated by the formula of 2000 divided by the corrosion rate in mil/year, which finds out only 3.5 days. Because the duration is too short, the test was conducted until deformation of the specimen was evident, which was 7 days. After 7 days, the

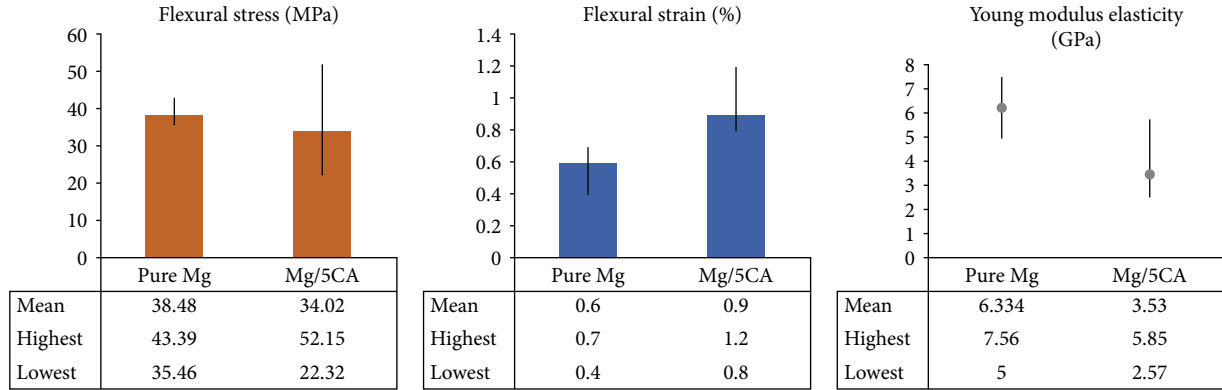


FIGURE 3: Biomechanical data of pure Mg specimen compared with Mg-5CA composite specimen. The error bars represent the standard deviation of measurements in three separate sample runs. Note: flexural stress of human bone: 133-295 MPa; flexural strain of human bone: 0.7-3.0%; flexural modulus elasticity of human bone: 15-35 GPa.

specimens were rubbed with sand grit paper and rinsed with acetone and alcohol to cleanse the corrosion products. The corrosion rate was calculated by using formula

$$\text{Corrosion rate} = \frac{(K \times W)}{A \times T \times D}, \quad (1)$$

where $K = \text{constant}$, $\text{mil per year (mpy)} = 3.45 \times 10^6$, $\text{millimeters per year (mm/y)} = 8.76 \times 10^4$, $T = \text{time of immersion (hour)}$, $A = \text{surface area (cm}^2\text{)}$, $W = \text{lost mass (gram)}$, and $D = \text{density (g/cm}^3\text{)}$.

2.5. Data Analysis. Data were analysed by using IBM SPSS Statistics 20. Distribution of the data was tested with Shapiro-Wilk. Normally distributed data were analysed by using two-way ANOVA, followed by post hoc Tukey. Abnormally distributed data were analysed by Kruskal-Wallis. Within-group analysis was also conducted by using a paired t -test if the data distribution is normal and with Mann-Whitney if the distribution is abnormal.

3. Results and Discussion

3.1. Composite Fabrication. The composite of magnesium and various content of carbonate apatite were successfully fabricated (Figure 1). More detailed data on the microstructure and microhardness of the specimen were discussed in our other publication [16]. Optical microscope analysis showed that the specimens have granule size between 150 and 451 microns. However, there was a high number of pores within the material (Figure 2).

Fabrication technique and parameters affect the resulted composite product. Some factors that may affect the process include material mixture ratio, milling time, the form of the specimen, fabrication method/technique, temperature, pressure, heating rate, and furnace atmosphere. The powder metallurgy method was chosen for this study because the technique has been shown to offer flexibility for design, homogeneous distribution, and capability to produce better mechanical properties despite the possibility of lower density material [17]. It is well acknowledged that in the casting process of Mg, a reaction with calcium phosphate may lead to

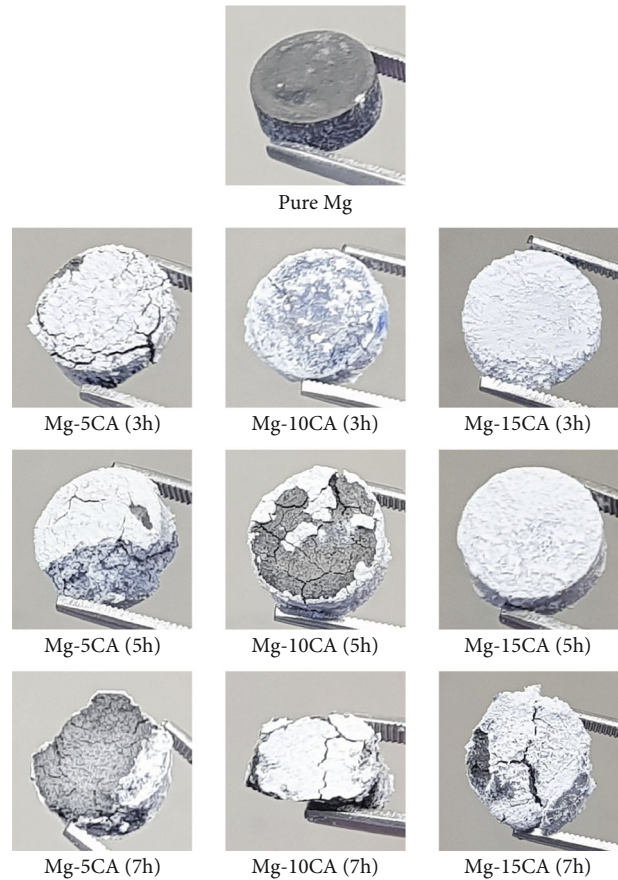


FIGURE 4: Appearance of the specimens after 6 days of immersion.

the formation of magnesium phosphide gas. Reaction with water could make the gas turn into a very toxic gas, the phosphine gas.

Carbonate apatite contents of 5%, 10%, and 15% were referring to the ratio that was used by Campo et al. [18], although the study used hydroxyapatite as its material. The parameters of vacuum drying were referred to parameters that were used by Gu et al. [19] The compaction pressure that we used was 265 MPa, which is also the ultimate tensile

TABLE 1: Results of the first indirect biocompatibility test.

Specimen	Survivability at 24 hours (\pm SD)	Survivability at 48 hours (\pm SD)	Survivability at 72 hours (\pm SD)
Blank media	0.000	0.000	0.000
Control media with cells only	100.000*	100.000*	100.000*
Pure magnesium	18.421 (\pm 0.153)	24.211	0.000
Mg-5CA 3 hours of milling time	56.316 (\pm 0.115)*	44.737 (\pm 0.147)	0.000 (\pm 0.174)
Mg-10CA 3 hours of milling time	70.000 (\pm 0.102)*	32.105 (\pm 0.127)	23.684 (\pm 0.176)
Mg-15CA 3 hours of milling time	85.263 (\pm 0.088)*	47.895 (\pm 0.139)	11.579 (\pm 0.148)
Mg-5CA 5 hours of milling time	4.211 (\pm 0.168)	53.684 (\pm 0.123)*	35.789 (\pm 0.161)
Mg-10CA 5 hours of milling time	35.263 (\pm 0.136)	63.158 (\pm 0.118)*	23.158 (\pm 0.136)
Mg-15CA 5 hours of milling time	0.000 (\pm 0.175)	44.211 (\pm 0.109)	44.737 (\pm 0.149)
Mg-5CA 7 hours of milling time	64.211 (\pm 0.108)*	6.842 (\pm 0.127)	0.000 (\pm 0.127)
Mg-10CA 7 hours of milling time	85.789 (\pm 0.088)*	14.737 (\pm 0.165)	0.000 (\pm 0.180)
Mg-15CA 7 hours of milling time	66.842 (\pm 0.105)*	36.316 (\pm 0.157)	0.000 (\pm 0.179)

Notes: Mg-(X)CA = composite of Mg containing x percent amount of CO_3Ap ; *survivability > 50% = not toxic.

TABLE 2: Results of the first direct contact test.

Specimen	Cell viability (%)
Control media with cells only	100.000*
Pure magnesium	4.348
Mg-5CA (milling time of 3 hours)	4.348
Mg-10CA (milling time of 3 hours)	4.348
Mg-15CA (milling time of 3 hours)	0.000
Mg-5CA (milling time of 5 hours)	4.348
Mg-10CA (milling time of 5 hours)	26.087
Mg-15CA (milling time of 5 hours)	0.000
Mg-5CA (milling time of 7 hours)	0.000
Mg-10CA (milling time of 7 hours)	0.000
Mg-15CA (milling time of 7 hours)	4.348

Notes: Mg-(X)CA = composite of Mg containing x percent amount of CO_3Ap ; *survivability > 50% = not toxic.

strength of Mg. Compaction temperature was 350°C , which is around half of the melting point of Mg (650°C).

Milling times of 3, 5, and 7 hours were adapted based on the interval choice in the study by Annur et al. [20], who chose 3, 5, and 8 hours as the milling time. The study found that the shorter the milling time, the smaller the particle size they were able to obtain. High risk of agglomeration is found on longer milling time. Unfortunately, we did not study the size of the particle. But we found that specimens with milling time of 5 hours have the least toxic effect. The relationship is thought that longer milling time would lead to agglomeration and induce the toxic effect, while faster milling time is not adequate to ensure uniform distribution of both materials, leading to low interparticle consolidation.

The problem of low interparticle consolidation is also thought to be related to the density of the specimen. We made the composite material in the form of a long cylinder block and cut it into small cylinders, which then would be

used as the specimen. The specimens that were used for the first biocompatibility tests were cut from the bottom side of the cylinder block, while the second biocompatibility tests' specimens were cut from the upper side. The upper side of the cylinder block is presumably to have a better density, as the area has direct contact with the hydraulic stamping. As it turns out, the second specimens had better toxicity profiles on the biocompatibility tests. We calculated the density of the similar specimens during the corrosion testing and found out that the specimens' density is equal with the bone's ($1.95\text{--}2.13\text{ g/cm}^3$ vs. $1.8\text{--}2.1\text{ g/cm}^3$). ASTM G31-72(2004) suggests that the specimens are cut from a sheet layer. This is to ensure that the materials are distributed more uniform in all areas. Unfortunately, our facility does not have the tools to cut specimens from sheet layers.

Particle size, density, and interparticle consolidation play important role in affecting the biomechanical properties, biocompatibility, corrosion product release, and degradability. All of these could be achieved better by applying a severe plastic deformation process during fabrication of the specimen. Some well-known techniques include extrusion and Equal Channel Angular Pressure (ECAP).

3.2. Biomechanical Testing. Data on flexural stress, flexural strain, and flexural modulus elasticity is presented in Figure 3. It was observed that the value of flexural stress and flexural modulus elasticity of our material is lower than that of the bone. On the contrary, the flexural strain is comparable with the bone's.

Good flexural strain, low flexural stress, and low Young modulus mean that the material may be dense enough, but it is brittle. Poor biomechanical properties of our specimens would also relate to the poor interparticle consolidation. Besides fabrication techniques, the oxidation process may also play a role in decreasing interparticle consolidation.

Magnesium is a metal that easily reacts with oxygen, forming $\text{Mg}(\text{OH})_2$. This oxidation reaction may be formed before processing (e.g., Mg powder is exposed to vapour or steam)

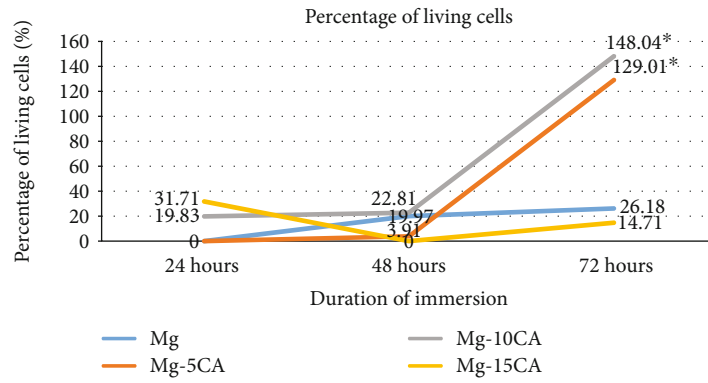


FIGURE 5: Percentage of living cells based on adjusted optical density on the second indirect biocompatibility test.

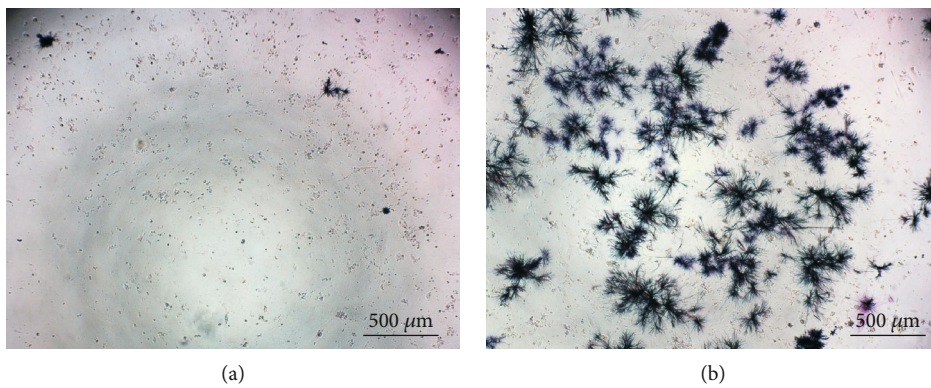


FIGURE 6: Optical microscope appearance of Mg-10CA specimen during indirect test: (a) first day of immersion; (b) after 6 days of immersion.

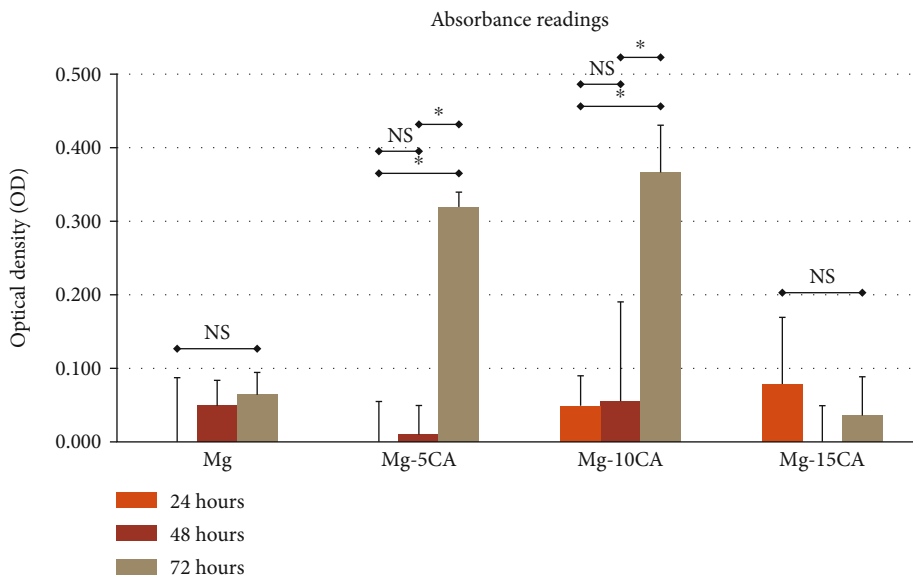


FIGURE 7: Statistical analysis on spectrophotometry absorbance readings. The error bars represent the standard deviation of measurements in three separate sample runs.

TABLE 3: Results of the second direct contact test.

Specimen	Cell viability (%)
Control media with cells only	87.5
Pure magnesium	0.000
Mg-5CA (milling time of 5 hours)	0.000
Mg-10CA (milling time of 5 hours)	66.667*
Mg-15CA (milling time of 5 hours)	0.000

Notes: Mg-(X)CA = composite of Mg containing x percent amount of CO_3Ap ; * survivability $> 50\%$ = not toxic.

and also the heating during the fabrication process. The formed stable oxide layer would impede the interparticle consolidation.

3.3. Biocompatibility Tests. Upon specimen immersion, some changes can be observed: disintegration after 48 hours of immersion, H_2 gas and corrosion product surrounding the specimen (Figure 4), and colour changes of the complete medium from reddish into purplish. The first batch of biocompatibility tests was done by using specimens that were cut from the bottom side of the composite cylinder block.

The first MTT test showed a reduction in the living cell population over time in almost all of the specimens (Table 1). Although specimens which were mixed for 5 hours showed a drastic decrease in spectrophotometer reading, the value increased at 48 hours and 72 hours. It can be inferred that material exposure elicits toxic reaction to the surrounding environment on the first day, and this toxic effect reduces over time.

The first direct contact test showed disintegration of the specimens and extensive release of corrosion product which covers the well surface. Our study found that all of our specimens were toxic. Composite of Mg with 10% content of CO_3Ap has the least toxicity (Table 2).

We repeated the biocompatibility test using specimens with the least toxic profile, which is the specimens that were mixed (milled) for 5 hours. Content of CO_3Ap was still varied (5%, 10%, and 15%).

The second MTT test showed that, upon spectrophotometry reading, the specimens of pure Mg and Mg with 15% content of CO_3Ap had a low living cell percentage based on adjusted optical density ($< 50\%$). On the other hand, specimens of Mg with 5% content of CO_3Ap and Mg with 10% content of CO_3Ap show high toxicity on the 24 hours and 48 hours of immersion. At 72 hours of immersion, these two specimens were shown as nontoxic (Figures 5 and 6).

These findings were also supported with statistical analysis, which showed a significant interaction between types of specimens and duration of immersion. Immersion for 72 hours showed the most significant result on two-way ANOVA compared with other duration of immersion. Additionally, Tukey post hoc analysis finds significant differences in the percentage of surviving cells on specimens of Mg with 5% content of CO_3Ap and Mg with 10% content of CO_3Ap compared to pure Mg (Figure 7).

The second direct contact test showed that specimens of Mg with 10% content of CO_3Ap had 66.67% of viable cells, and thus, the composite was not toxic (Table 3, Figure 8).

Our study found that the composite of Mg with 10% content of CO_3Ap mixed for 5 hours is the least toxic specimen. An unusual phenomenon can be observed in our specimens. Composite specimens which have been mixed for 3 hours and 7 hours follow common phenomena of toxic material, i.e., least toxic at the beginning of exposure, but the longer the exposure, the more toxic it is. On the other hand, composite specimens which have been mixed for 5 hours showed otherwise: most toxic in the first 24 hours of exposure, but it becomes less toxic later on.

Our study used the MTT colourimetric test due to its sensitivity in detecting indirect cytotoxicity. The MTT assay and neutral red uptake assay are the most sensitive to detect cytotoxicity compared with the LDH assay and protein assay [21]. We also used UC-MSCs as the subject cells for biocompatibility tests. The use of bone marrow stem cells (BM-MSCs) should be better because it would represent a similar condition of the cells surrounding the area of the fracture.

The unique pattern of cell viability on the composite of Mg with 10% content of CO_3Ap might be contributed by two factors. The first factor is the tetrazolium-based MTT reagent. Metabolic activity of living cells would induce reduction reaction towards tetrazolium, forming formazan crystal. Unfortunately, the result of the test could be biased if the substance or material that is tested also have reductant characteristic.

Magnesium reacts easily with atmospheric air forming $\text{Mg}(\text{OH})_2$ layer and H_2 by-product. Additionally, the oxide layer would produce 2OH^- by-product when exposed to chloride ion, which is commonly found on body fluid, including on the complete medium that we used. These hydrogen and hydroxide by-products are reductant substances. Its release would also induce formazan crystal formation and increase optical density reading on spectrophotometry, leading to a false-positive result:



The second possible factor is that the MTT assay cannot differentiate between cytotoxic and cytostatic [22]. Similar to Zhao et al. [23], it is arguable that there is a possibility where specimen exposure does not cause cell/gene membrane damage or even cell death. Nevertheless, it only decreases metabolic activity or changes in gene regulation. To study this matter further, direct manual observation on cell morphology is needed by using an optical microscope or scanning electron microscope (SEM).

Some factors may bias the result of direct exposure testing. Subjectivity upon direct microscope observation is one factor. Another factor is the small amount of medium that was taken and stained with trypan blue to represent the cell population. Living cells may not be included in the samples. Additionally, the size of our specimen occupies approximately 50% of the well surface. Additional corrosion by-product would even occupy more of the well plate surface,

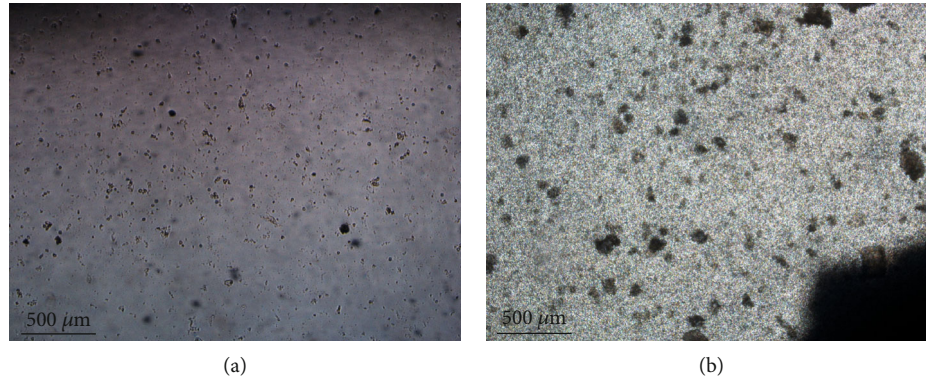


FIGURE 8: Optical microscope appearance of Mg-10CA specimen during direct contact test: (a) first day of immersion; (b) after 2 days of immersion.

TABLE 4: Characteristics of specimens on the biocorrosion test.

Specimen	Weight decrease (g)	Posttest pH	Corrosion rate (mpy)	Corrosion rate (mm/year)	Density (g/cm ³)
Pure Mg	0.0988	9.09	164.2405	4.1702	1.9661
Mg-5CA	0.2874	9.81	799.7770	20.3071	1.9575
Mg-10CA	0.2717	9.84	448.6945	11.3929	1.9791
Mg-15CA	0.1110	9.81	226.8837	5.7608	2.1320

Notes: Mg-(X)CA = composite of Mg containing x percent amount of CO₃Ap.

limiting space for the cells to proliferate. This condition would lead to false-negative results.

The problem is similar to the study done by Zhao et al. [23] who also studied magnesium stent in a static environment similar to our method. Different from our testing condition, the actual *in vivo* environment is dynamic. Cells would have a larger space to occupy and attach to. Dynamic circulation of blood and body fluids would also play important roles in removing degradation product of Mg and in preventing the drastic increase of pH.

3.4. Biocorrosion Test. The corrosion test was done by immersing the specimen until deformity was noted. On the seventh day, split or disintegration of Mg with 5% content of CO₃Ap and Mg with 10% content of CO₃Ap was observed. Thus, the test was stopped. The pH level of the DMEM before the test was set to 7.15. The characteristics of the specimens before and after are presented in Table 4. The test revealed that after 7 days of immersion, all of the specimens decreased in weight. The smallest decrease was observed on pure Mg, followed by Mg with 15% content of CO₃Ap. A similar manner was also observed in the value of the corrosion rate.

Some factors determining the outcome of corrosion testing are types of medium, static/dynamic condition, atmosphere environment, and duration of immersion. We chose DMEM as the medium in accordance with the systematic review by Gonzalez et al. [14] The authors stated that when DMEM is used in cell culture condition, it can maintain physiological pH and degradation layer, similar to *in vivo* condition. Unfortunately, due to the limited facility, we cannot regulate and maintain a suitable environment for cell

culture conditions (5% CO₂, 2% O₂, humidity 95%, and temperature $\pm 1^\circ\text{C}$).

We suspended the corrosion testing on day seven, due to the significant disintegration of the test samples. The corrosion rate decrease along with the increasing content of carbonate apatite. Ding stated that the ideal orthopaedic biodegradable material should have a degradation rate of less than 0.5 mm/year [6]. The corrosion rates of our specimen are still far from this requisite. The high corrosion rate of our specimens is mainly caused by poor interparticle consolidation.

3.5. Acidity Level. On the other hand, the pH of DMEM after the immersion test was found to be ranged at 9.0-9.8. As shown in Figure 9, the colour of DMEM medium changes from ruby red to purplish pink, which signifies an alkaline environment. An additional characteristic that we were able to calculate is density. Our specimens have a good density of 1.95-2.13 g/cm³.

After 7 days of immersion, the medium pH of our specimens was altered into the range of 9.0-9.8. The known optimal pH value for cell culture condition is 7.2-7.5. However, this condition would be different *in vivo*, especially its effect on soft tissue healing and bone healing. Kruse et al. studied the activity of migration, proliferation, and viability of keratinocyte and fibroblasts during wound healing and its relationship with the acidity level [24]. They found that proliferation of both cells, especially fibroblasts, is increasing in an alkali environment. They also stated that the alkali environment does not have a negative side effect towards wound reepithelialization, even tending to be increased. The level of IL-1 α , one of the inflammation factors, is also found not increased in alkali environment.



FIGURE 9: Colour changes of the DMEM from red (a) into purplish pink (b) signify alkali environment after specimen immersion.

In regard to bone healing, the activity of osteoclast is known best at neutral pH but stops at pH of 7.4 [25]. Systemic acidosis has a negative side effect towards bone mineralization, increase osteoclast activity, and prevent osteoblast activity. On the other hand, systemic metabolic alkalosis decreases bone resorption and stimulate osteoblasts' collagen synthesis [26]. One study by Galow et al. [27] found that osteoblast proliferation reaches its peak at pH of 8.0-8.4. However, its relationship between the alkali environment and overall bone healing process needs to be studied further.

4. Conclusions and Suggestions for Future Studies

Fabrication of the magnesium-carbonate apatite composite is feasible, and it is a potential new biodegradable orthopaedic implant material. Our study revealed that the composite of Mg with 10% content of CO_3Ap has good biocompatibility despite its biomechanical properties and degradation rate being lesser than the desired standard. The key to improve those properties is by improving interparticle consolidation, which can be achieved by further study and modification of the fabrication method.

Our study has some weaknesses in terms of methodology. However, from these weaknesses, we were able to compile some important factors that must be considered when studying magnesium composite for biodegradable materials.

Our study fails to follow ASTM standards including the form of specimens, testing condition, and controlled environment condition (ASTM E290-14 for the bending test, ASTM G31-72(2004) for corrosion testing). Additionally, less oxygen exposure towards magnesium (such as the use of vacuum storage, vacuum furnace, and irradiation sterilization method) is preferable to prevent excessive oxidation of magnesium.

Fabrication methods such as fast sintering (spark plasma sintering), low-temperature sintering, severe plastic deformation processing (e.g., extrusion and ECAP), coating, or micro-arc oxidation may improve the interparticle consolidation.

In terms of test materials, bone marrow mesenchymal stem cells should be used. Alkali phosphatase activity may also be measured to determine the behaviour of bone cells. An alternative colourimetric assay other than the MTT assay should be considered (e.g., neutral red uptake assay, sulforhodamine B assay, and crystal violet assay). Additionally, cell morphology direct observation under an optical microscope or SEM may also give more accurate condition.

Data Availability

The data used to support the findings of this study are available from the corresponding author upon request.

Disclosure

Our preliminary study was presented at Second International Symposium on Biomedical Engineering (ISBE) 2018 and published at AIP Conference Proceedings 2092 [1]:020021 (DOI: 10.1063/1.5096689).

Conflicts of Interest

The authors declare that there is no conflict of interest regarding the publication of this paper. The authors certify that they have no affiliation or involvement with companies whose products are featured in the study or any other organization or company with financial interest and nonfinancial interest in the subject matter or materials discussed in this manuscript. No human participant or animal testing was performed in this study.

Acknowledgments

This study is funded by the International Indexed Publications for Student Final Project (PITTA) grant by Universitas Indonesia and Higher Education Featured Basic Research (PDUPT) grant by Indonesian Ministry of Research Technology and Higher Education (Kemenristekdikti) (Contract Number. 312/UN2.R3.1/HKP05.00/2018).

References

- [1] H. Karimi-Maleh, S. Ranjbari, B. Tanhaei et al., "Novel 1-butyl-3-methylimidazolium bromide impregnated chitosan hydrogel beads nanostructure as an efficient nanobio-adsorbent for cationic dye removal: kinetic study," *Environmental Research*, vol. 195, article 110809, 2021.
- [2] M. Navarro, A. Michiardi, O. Castano, and J. A. Planell, "Bio-materials in orthopaedics," *Journal of the Royal Society Interface*, vol. 5, no. 27, pp. 1137-1158, 2008.
- [3] A. J. Rahyussalim, A. F. Masetio, I. Saleh, T. Kurniawati, and Y. Whulanza, "The needs of current implant technology in orthopaedic prosthesis biomaterials application to reduce prosthesis failure rate," *Journal of Nanomaterials*, vol. 2016, Article ID 5386924, 9 pages, 2016.
- [4] J. Nagels, M. Stokdijk, and P. M. Rozing, "Stress shielding and bone resorption in shoulder arthroplasty," *Journal of Shoulder and Elbow Surgery*, vol. 12, no. 1, pp. 35-39, 2003.

- [5] H. Park, J. Temenoff, and A. Mikos, "Biodegradable orthopedic implants," in *Engineering of Functional Skeletal Tissues*, F. Bronner, M. C. Farach-Carson, and A. G. Mikos, Eds., pp. 55–68, Springer, London, 2007.
- [6] W. Ding, "Opportunities and challenges for the biodegradable magnesium alloys as next-generation biomaterials," *Regenerative Biomaterials*, vol. 3, no. 2, pp. 79–86, 2016.
- [7] Y. Akiko, "Biomedical application of magnesium alloys," *Journal of Japan Institute of Light Metals*, vol. 58, pp. 570–576, 2008.
- [8] M. P. Staiger, A. M. Pietak, J. Huadmai, and G. Dias, "Magnesium and its alloys as orthopedic biomaterials: a review," *Biomaterials*, vol. 27, no. 9, pp. 1728–1734, 2006.
- [9] Y. Ayukawa, Y. Suzuki, K. Tsuru, K. Koyano, and K. Ishikawa, "Histological comparison in rats between carbonate apatite fabricated from gypsum and sintered hydroxyapatite on bone remodeling," *BioMed Research International*, vol. 2015, Article ID 579541, 7 pages, 2015.
- [10] American Society for Testing and Materials, *ASTM E290-14 standard test methods for bend testing of material for ductility*, pp. 1–8, ASTM International, 2014.
- [11] J. A. Pawitan, I. K. Liem, E. Budiyantri et al., "Umbilical cord derived stem cell culture: multiple-harvest explant method," *International Journal of PharmTech Research*, vol. 6, no. 4, pp. 1202–1208, 2014.
- [12] T. Mosmann, "Rapid colorimetric assay for cellular growth and survival: application to proliferation and cytotoxicity assays," *Journal of Immunological Methods*, vol. 65, no. 1-2, pp. 55–63, 1983.
- [13] American Society for Testing and Materials, *ASTM G31-72 (2004). Standard practice for laboratory immersion corrosion testing of metals*, pp. 1–8, ASTM International, 2004.
- [14] J. Gonzalez, R. Q. Hou, E. P. S. Nidadavolu, R. Willumeit-Romer, and F. Feyerabend, "Magnesium degradation under physiological conditions - best practice," *Bioactive Materials*, vol. 3, no. 2, pp. 174–185, 2018.
- [15] L. Liu, K. Gebresellasie, B. Collins et al., "Degradation rates of pure zinc, magnesium, and magnesium alloys measured by volume loss, mass loss, and hydrogen evolution," *Applied Sciences*, vol. 8, no. 9, p. 1459, 2018.
- [16] I. Setyadi, A. F. Marsetio, A. F. Kamal, A. J. Rahyussalim, S. Supriadi, and B. Suharno, "Microstructure and microhardness of carbonate apatite particle-reinforced Mg composite consolidated by warm compaction for biodegradable implant application," *Materials Research Express*, vol. 7, no. 5, article 056526, 2020.
- [17] K. Kusnierczyk and M. Basista, "Recent advances in research on magnesium alloys and magnesium-calcium phosphate composites as biodegradable implant materials," *Journal of Biomaterials Applications*, vol. 31, no. 6, pp. 878–900, 2017.
- [18] R. D. Campo, B. Savoini, A. Munoz, M. A. Monge, and G. Garces, "Mechanical properties and corrosion behavior of Mg-HAP composites," *Journal of the Mechanical Behavior of Biomedical Materials*, vol. 39, pp. 238–246, 2014.
- [19] X. Gu, W. Zhou, Y. Zheng, L. Dong, Y. Xi, and D. Chai, "Microstructure, mechanical property, bio-corrosion and cytotoxicity evaluations of Mg/HA composites," *Materials Science and Engineering: C*, vol. 30, no. 6, pp. 827–832, 2010.
- [20] D. Annur, A. Suhardi, M. I. Amal, M. S. Anwar, and I. Kartika, "Powder metallurgy preparation of Mg-Ca alloy for biodegradable implant application," *Journal of Physics Conference Series*, vol. 817, no. 1, pp. 1–6, 2017.
- [21] G. Fotakis and J. A. Timbrell, "In vitro cytotoxicity assays: comparison of LDH, neutral red, MTT and protein assay in hepatoma cell lines following exposure to cadmium chloride," *Toxicology Letters*, vol. 160, no. 2, pp. 171–177, 2006.
- [22] J. A. Plumb, "Cell sensitivity assays: the MTT assay," *Methods in Molecular Medicine*, vol. 88, pp. 165–169, 2004.
- [23] N. Zhao, N. Watson, Z. Xu et al., "In vitro biocompatibility and endothelialization of novel magnesium-rare earth alloys for improved stent applications," *PLoS One*, vol. 9, no. 6, article e98674, 2014.
- [24] C. R. Kruse, M. Singh, S. Targosinski et al., "The effect of pH on cell viability, cell migration, cell proliferation, wound closure, and wound reepithelialization: in vitro and in vivo study," *Wound Repair and Regeneration*, vol. 25, no. 2, pp. 260–269, 2017.
- [25] T. R. Arnett, "Extracellular pH regulates bone cell function," *The Journal of Nutrition*, vol. 138, no. 2, pp. 415S–418S, 2008.
- [26] D. A. Bushinsky, "Acid-base imbalance and the skeleton," *European Journal of Nutrition*, vol. 40, no. 5, pp. 238–244, 2001.
- [27] A. M. Galow, A. Rebl, D. Koczan, S. M. Bonk, W. Baumann, and J. Gimsa, "Increased osteoblast viability at alkaline pH in vitro provides a new perspective on bone regeneration," *Biochemistry and Biophysics Reports*, vol. 10, pp. 17–25, 2017.